

Resonance capacity of surface plasmon on subwavelength metallic structures

YING GU^(a), LIANGLIANG CHEN, HAIXI ZHANG and QIHUANG GONG^(b)

State Key Laboratory for Mesoscopic Physics, Department of Physics, Peking University - Beijing 100871, China

received 21 April 2008; accepted in final form 28 May 2008

published online 27 June 2008

PACS 73.20.Mf – Collective excitations (including excitons, polarons, plasmons and other charge-density excitations)

PACS 78.67.-n – Optical properties of low-dimensional, mesoscopic, and nanoscale materials and structures

PACS 78.68.+m – Optical properties of surfaces

Abstract – Green’s matrix method as well as the newly defined resonance capacity of surface plasmon are presented and applied to select the strong resonances for arbitrary shaped subwavelength metallic structures. The resonance capacity distributions for a certain structure type make it possible to tailor the metallic resonant properties in the selected wavelength. Moreover, the resonance capacity is found to be almost immune to the incident wavelength for a definite structure zoomed in or out in the subwavelength scale ($l < \frac{\lambda}{15}$). Our numerical calculations are also in agreement with the previous experimental results on nanoantennas.

Copyright © EPLA, 2008

The near field concerns the evanescent wave bound to a nanostructured material surface which decays exponentially within the range of wavelength [1,2]. At the interface of metal and dielectric or in the isolated metallic nanostructures, due to the collective oscillations of free electrons, surface plasmons [3–5] are excited, accompanied with the enhancement of the optical near field. This resonant enhancement has promoted many important applications, such as surface-enhanced Raman scattering [6], optical antenna [7], and optical frequency mixing [8–10]. Based on the coupling of the optical near field at resonance, below the light diffraction limit, nanometer plasmonic waveguide [11] and biosensor [12,13] with gold nanoparticles were demonstrated. The near-field intensity directly affects these fundamental applications and the efficiency of nanodevices. The larger near field at the surface comes from the larger electric field carried by the metal ($\epsilon_d E_{d\perp} = \epsilon_m E_{m\perp}$), which may be optimized by well matching the geometry, incident light, metallic electric permittivity and dielectric environment.

The Green’s tensor method [14] has successfully solved the optical near field of the isolated nanostructures, yet the information on surface plasmon resonance is not explicitly provided. In this letter, by combining the Green’s tensor method with Green’s function formalism in the quasistatic

limit [15], we developed the Green’s matrix method to deal with the surface plasmon resonance and the near field of the arbitrary shaped subwavelength metallic structures. The new physical variable, the resonance capacity of surface plasmon, is defined to quantitatively measure the electromagnetic energy gathered from the environment. Using the resonance capacity, we can select those strong resonances in a subwavelength cluster. For example, the experimental results of nanoantennas [7] are well demonstrated. The resonance capacity distributions for a certain structure type make it possible to tailor the metallic resonant properties in the selected wavelength. We found that the strong resonances in the rectangular structures are regularly shifted with the geometrical parameters and field polarization, then the resonant nanostructures of a noble metal in the visible are designed. For a definite structure zoomed in or out in the subwavelength region $l < \frac{\lambda}{15}$, its resonance capacity distribution is not sensitive to the incident wavelength. The method should provide a new measure in the plasmonic optics and device design.

Consider an arbitrary shaped subwavelength structure with the electric permittivity $\epsilon(\mathbf{r}, \omega)$ embedded in an homogeneous bulk material with $\epsilon_0(\omega)$. These subwavelength clusters are not necessarily connected, but the tensor $\epsilon_s(\mathbf{r}, \omega) (= \epsilon(\mathbf{r}, \omega) - \epsilon_0(\omega))$ vanishes outside the clusters. The electric permittivity $\epsilon(\mathbf{r}, \omega)$ is complex and frequency dependent in real metal. If a monochromatic incident field $E^0(\mathbf{r})$ (with the usual $e^{-i\omega t}$ time dependence

^(a)E-mail: ygu@pku.edu.cn

^(b)E-mail: qhgong@pku.edu.cn

throughout this paper) impinges on the system, without any approximation of Maxwell equations, the scattered field $E(\mathbf{r})$ is a solution of the propagation equation

$$-\nabla \times \nabla \times E(\mathbf{r}) + k^2 \epsilon_0(\omega) E(\mathbf{r}) + k^2 \epsilon_s(\mathbf{r}, \omega) E(\mathbf{r}) = 0 \quad (1)$$

where k is the vacuum wave number. With Green's tensor in a three-dimensional system [16]

$$G^0(\mathbf{r}, \mathbf{r}', \omega) = \left(\mathbf{I} - \frac{1 - ik_0 R}{k_0^2 R^2} \mathbf{I} - \frac{-3 + 3ik_0 R + k_0^2 R^2}{k_0^2 R^4} \mathbf{R}\mathbf{R} \right) \frac{\exp[ik_0 R]}{4\pi R}, \quad (2)$$

where $R = |\mathbf{R}| = |\mathbf{r} - \mathbf{r}'|$ and $k_0^2 = k^2 \epsilon_0(\omega)$, the field $E(\mathbf{r})$ at any point \mathbf{r} satisfies the Lippmann-Schwinger equation [14, 17]

$$E(\mathbf{r}) = E^0(\mathbf{r}) + k^2 \int_V d\mathbf{r}' G^0(\mathbf{r}, \mathbf{r}', \omega) \epsilon_s(\mathbf{r}', \omega) \cdot E(\mathbf{r}'), \quad (3)$$

where V denotes the clusters subspace. Replacing the traditional matching of the boundary conditions with the self-consistent coupling of all source points makes the Green's tensor method a powerful tool in dealing with various geometrically complex and subwavelength materials [1]. It has been successfully extended to the problems with different boundary conditions [18–21]. The divergence of Green's tensor $G^0(\mathbf{r}, \mathbf{r}', \omega)$ is handled by the regularization scheme [22].

If the clusters subspace V is divided into N pieces with the volume δV (with $\delta V \ll V$), eq. (3) becomes

$$\sum_{\mathbf{r}' \in V} [\epsilon_s(\mathbf{r}, \omega) \tilde{G}^0(\mathbf{r}, \mathbf{r}', \omega) - \delta_{\mathbf{r}, \mathbf{r}'}] \tilde{E}(\mathbf{r}) = -\tilde{E}^0(\mathbf{r}) \quad (4)$$

with $\tilde{G}^0(\mathbf{r}, \mathbf{r}', \omega) = \delta V k^2 G^0(\mathbf{r}, \mathbf{r}', \omega)$. Let us rewrite it in the form

$$\sum_{\mathbf{r}' \in V} [\tilde{G}^0(\mathbf{r}, \mathbf{r}', \omega) - sI] \tilde{E}(\mathbf{r}) = \frac{-\tilde{E}^0(\mathbf{r})}{\epsilon_s(\mathbf{r}, \omega)}, \quad (5)$$

where $s = \frac{1}{\epsilon(\mathbf{r}, \omega) - \epsilon_0(\omega)}$. \tilde{G}^0 , a $3N \times 3N$ matrix, is called Green's matrix. Because \tilde{G}^0 is symmetrical, mathematically, there are $3N$ real eigenvalues. Physically, only those eigenvalues with the large residue of electric field correspond to the strong resonances. Then, in the following resonance capacity definition, we select these strong resonances by keeping the residues of $|E|^2$. So, in the numerical calculations, the mathematical eigenvalues depend on the numerical discretization, while the physical resonances do not. The region of the eigenvalue s_n is about $(-1.1, 0.1)$ according to our numerical results, so most of the eigen electric permittivities $\epsilon_n(r, \omega) (= \frac{1}{s_n} + \epsilon_0(\omega))$ fall into the negative real axis and cover the region of noble metals in the optical region. It is not an accident that eigen electric permittivities $\epsilon_n(r, \omega)$ have negative values. Physically, the cooperation of positive permittivity (here $\epsilon_0 = 1.0$) and

negative permittivity leads to the resonances of surface plasmon. Beyond the quasistatic limit where resonances are determined by the electric permittivities of clusters and reference media [15], when the retardation effect is considered, resonances are also explicitly related to the wave number k (included in \tilde{G}^0).

The electric field $\tilde{E}(\mathbf{r})$, a $3N \times 1$ matrix, in the clusters subspace has the general form

$$\tilde{E}(\mathbf{r}) = \sum_{n=1}^{3N} A_n(s) \cdot R_n, \quad (6)$$

where R_n is the right eigenvector of the n -th eigenvalue of \tilde{G}^0 . By substituting eq. (6) into eq. (5) and multiplying the left eigenvector $L_n (= R_n^T)$, $\tilde{E}(\mathbf{r})$ reads

$$\tilde{E}(\mathbf{r}) = \sum_{n=1}^{3N} \frac{s L_n \cdot \tilde{E}^0(\mathbf{r})}{(s - s_n)} \cdot R_n. \quad (7)$$

For any point \mathbf{r} outside the nanoclusters, we have

$$E(\mathbf{r}) = E^0(\mathbf{r}) + k^2 \sum_{n=1}^{3N} \frac{L_n \cdot \tilde{E}^0(\mathbf{r})}{(s - s_n)} \cdot \left[\sum_{\mathbf{r}' \in C} G^0(\mathbf{r}, \mathbf{r}', \omega) \cdot R_n \right]. \quad (8)$$

Hence, the near field as well as the far field can be analytically expressed by the Green's tensor $G^0(\mathbf{r}, \mathbf{r}', \omega)$, and eigenvalues s_n , eigenvectors R_n, L_n of Green's matrix \tilde{G}^0 .

Without loss, when s approaches one of the eigenvalues s_n , *i.e.*, $s \rightarrow s_n$, the electric fields diverge to infinity. Mathematically, there are $3N$ poles in the eigenvalue region $s \in (-1.1, 0.1)$, while only those eigenstates (or resonances) with strong near electric field are meaningful in physics and have some applications [6–13]. To select those resonances, we define the resonance capacity in view of the inside electric-field energy of the nanostructures. For each s_n , its resonance capacity is

$$C_n = \frac{\int_V d\mathbf{r}' |\epsilon_n| \cdot [\text{res}|E(\mathbf{r}')|]_n^2}{\int_V d\mathbf{r}' |\epsilon_0(\omega)| \cdot |E^0(\mathbf{r}')|^2} \quad (9)$$

with the residue of field $[\text{res}|E(\mathbf{r}')|]_n = |\frac{L_n \cdot \tilde{E}^0(\mathbf{r}')}{\epsilon_n(\mathbf{r}, \omega)} \cdot R_n|$ and $\epsilon_n = \frac{1}{s_n} + \epsilon_0(\omega)$. The value of C_n quantitatively expresses the ability to gather the electromagnetic energy from the environment for free electrons in metals. From the continuous boundary condition between the dielectric and the metal ($\epsilon_d E_{d\perp} = \epsilon_m E_{m\perp}$), we can find that the larger C_n means the larger value of $\epsilon_m E_{m\perp}$, so the more enhanced near field $E_{d\perp}$. So the resonance capacity can also provide the information about the dielectric constant of metal at resonance. Most importantly, by means of the resonance capacity, we can not only select those resonances with the strong near fields, but also quantitatively compare the resonance ability among various subwavelength structures. Conceptually, the extinction peaks of the far field should

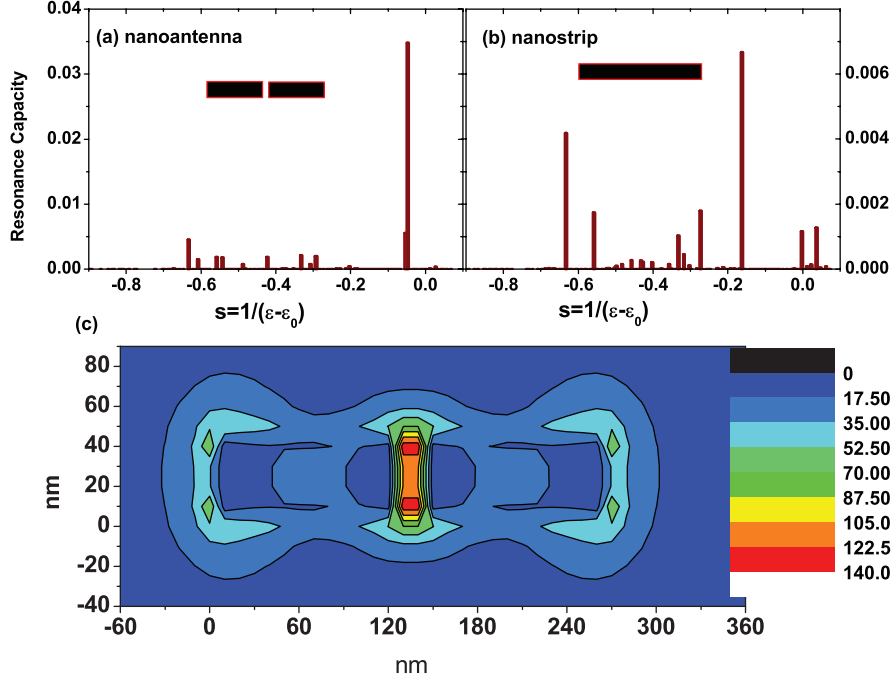


Fig. 1: (Color online) (a) Positions and capacity of the surface plasmon resonance for the nanoantenna with length 260 nm at 830 nm. (b) Positions and capacity of the surface plasmon resonances for the nanostrip with length 260 nm at 830 nm. (c) Optical-near-field distribution of the nanoantenna.

Table 1: Resonance positions and capacity for a set of optical nanoantennas.

Length L (nm)	SPR s	RC C_s	Dielectric constant ϵ
200	-0.0825	0.06494	-11.121
220	-0.0675	0.05449	-13.815
240	-0.0575	0.04464	-16.391
260	-0.0475	0.03483	-20.053
280	-0.0375	0.02447	-25.667
300	-0.0325	0.02791	-29.768
320	-0.0275	0.01541	-35.364
340	-0.0225	0.01457	-43.444

correspond to those resonances with high values of resonance capacity if only absorption is considered.

There is an essential difference between the Green's tensor method [14] and the Green's matrix method. In the Green's tensor method, the near field is explicitly expressed for the given parameters including the incident wavelength, geometry and dielectric constant of subwavelength clusters, while, in our Green's matrix method, only the incident wavelength and cluster geometry are given, then the resonant properties with respect to the dielectric constant of subwavelength clusters can be directly obtained. Rather than solving a set of linear equations in the Green's tensor method, here the core of the Green's matrix method is to solve the eigenvalues and eigenvectors of Green's matrix, so that the eigen properties of the

system can be expressed. It is known that the Mie theory can only deal with the optical responses of the subwavelength sphere and spherical symmetry clusters [23]. Principally, the union of the Green's matrix method and resonance capacity can select those resonances with strong near field in an arbitrary shaped subwavelength structure, which is more general and physical.

Using the Green's matrix method and resonance capacity, the experimental result of nanoantennas [7] is demonstrated successfully. The numerical calculations (we always let $\epsilon_0(\omega)=1.0$) on the nanoantennas and nanostrips are performed at the wavelength $\lambda=830$ nm with the length $L=200-340$ nm, feed gap of 20 nm, and transverse area of 40×40 nm², in steps of 10 nm. As shown in the table 1, for an antenna with $L=260$ nm ($s=-0.0475$ ($\epsilon(r,\omega)=-20.053$)) or 280 nm ($s=-0.0375$ ($\epsilon(r,\omega)=-25.667$)), there is a large resonance peak, corresponding to the dielectric constant region of Au around $\lambda=830$ nm, as shown in fig. 1(a). While for the same length strip in fig. 1(b), the resonance occurs at $s=-0.15$ ($\epsilon(r,\omega)=-5.667$). This value does not belong to the dielectric constant region of Au at this wavelength, so no resonance is observed. The capacity of resonance in the antenna is 5 times larger than that in strip. Immediately, fig. 1(c) displays the optical-near-field distribution of the nanoantenna with $L=260$ nm, $s=-0.0475$. The electric fields are highly concentrated within the gap, in good agreement with the experimental results [7]. We noted that the electric permittivity -20.053 at $L=260$ nm does not exactly equal $-25.3 + 1.6i$ [24] of Au at $\lambda=830$ nm. The main

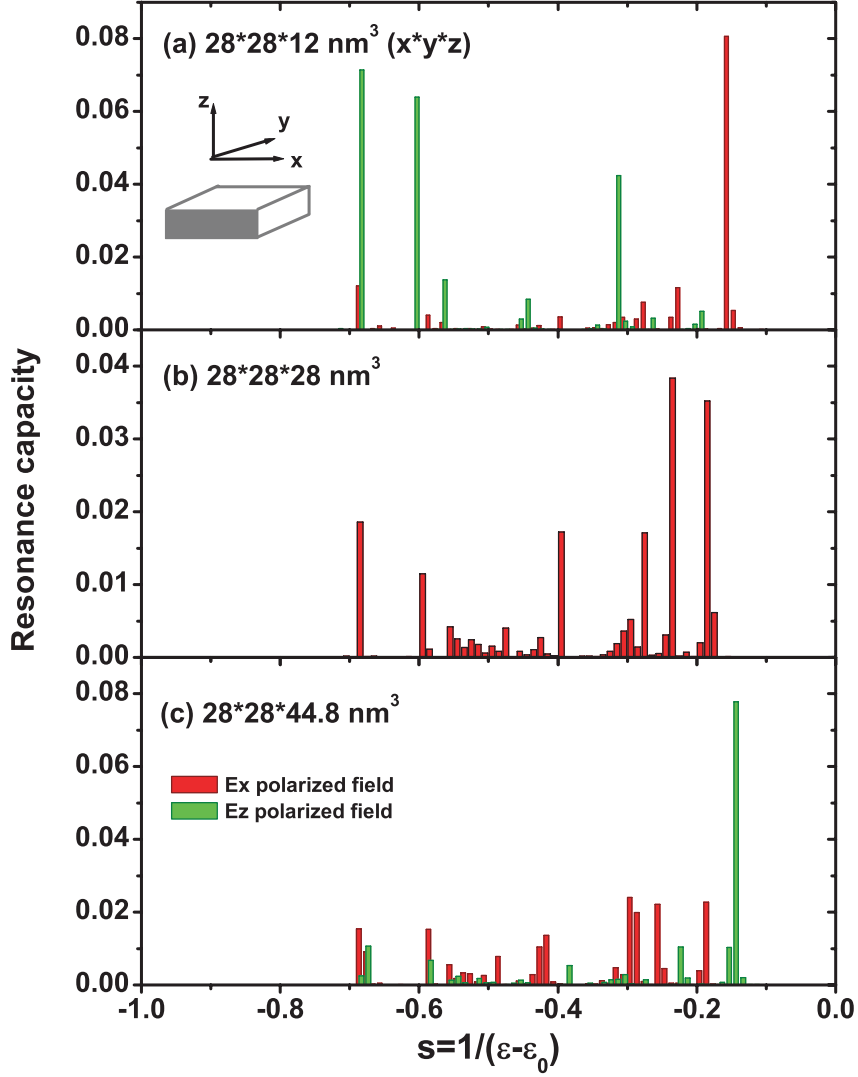


Fig. 2: (Color online) Resonance capacity of a set of rectangular subwavelength structures at 632.8 nm with E_x polarized field and E_z polarized field.

reason is the loss originated from the collisions between electrons and metallic ions and the spatial confinement in real metallic nanostructures (the electron mean free path for bulk gold is about 42 nm), which was also discussed in the analytic result of the Mie theory [23]. Further numerical calculations indicate that the position of the surface plasmon resonance is very sensitive to the transverse area and feed gap of nanoantennas.

Using the proposed method, the resonance capacity for a certain structure type can be obtained and it makes it possible to tailor the metallic resonant properties in the selected wavelength. In the following, as an example, we have explored the rectangular-type subwavelength metallic structures ($l < \frac{\lambda}{15}$) at the wavelength $\lambda = 632.8$ nm. The rectangle clusters have the area of 28 nm * 28 nm ($x * y$) and the height (z) from 8 nm to 56 nm. The E_x and E_z polarized electric fields are applied to excite the different direction of resonances (see the inset in fig. 2(a)). Here, the mesh in the calculations is $[2 \text{ nm}]^3$ or $[2.8 \text{ nm}]^3$ and

Table 2: Resonance positions and capacity for a set of optical nanostrips.

$x * y * z$ (nm ³)	Positions of SPR s	Resonance capacity C_s	Dielectric constant ϵ
90 * 30 * 12	-0.0375	0.03101	-25.667
90 * 30 * 15	-0.0475	0.03652	-20.053
90 * 30 * 18	-0.0525	0.04268	-18.048
90 * 30 * 21	-0.0575	0.04349	-16.391
90 * 30 * 24	-0.0625	0.05036	-15.000
90 * 30 * 27	-0.0675	0.05402	-13.815
90 * 30 * 30	-0.0725	0.05673	-12.793
90 * 21 * 12	-0.0275	0.02479	-35.364
90 * 21 * 18	-0.0425	0.03435	-22.529
90 * 21 * 21	-0.0475	0.03782	-20.053

$\epsilon_0(\omega) = 1.0$. Figure 2 displays the resonance capacity distributions of different rectangular structures and polarized fields. For a 28 * 28 * 28 nm³ cube, there are

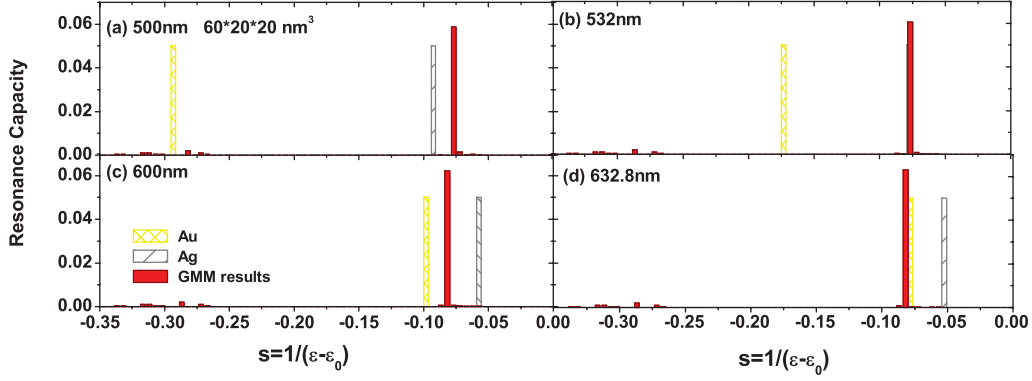

 Fig. 3: (Color online) Resonance capacity of the nanostrip $60 * 20 * 20 \text{ nm}^3$ from the wavelength 500 nm to 632.8 nm.

Table 3: Comparison between the discrete dipole approximation and the Green's matrix method results.

Nano structures	Discrete dipole approximation [26]		Green's matrix method	
	$V - 4\pi(r_{\text{eff}})^3/3$		$V = ab^2, R = a/b$	
	Dimensions	$\lambda_{\text{max}}(\text{nm})$	Dimensions	$\lambda_{\text{max}}(\text{nm})$
Nanorod 1	$R = 3.1$	727	$a = 39.17 \text{ nm}$	690
	$r_{\text{eff}} = 11.43 \text{ nm}$		$b = 12.64 \text{ nm}$	
Nanorod 2	$R = 3.9$	797	$a = 45.65 \text{ nm}$	760
	$r_{\text{eff}} = 11.43 \text{ nm}$		$b = 11.71 \text{ nm}$	
Nanorod 3	$R = 4.6$	863	$a = 50.96 \text{ nm}$	810
	$r_{\text{eff}} = 11.43 \text{ nm}$		$b = 11.08 \text{ nm}$	
Nanorod 4	$R = 3.9$	788	$a = 34.91 \text{ nm}$	745
	$r_{\text{eff}} = 8.74 \text{ nm}$		$b = 8.95 \text{ nm}$	
Nanorod 5	$R = 3.9$	815	$a = 71.49 \text{ nm}$	790
	$r_{\text{eff}} = 17.90 \text{ nm}$		$b = 18.33 \text{ nm}$	
Nanorod 6	$R = 3.9$	842	$a = 87.31 \text{ nm}$	810
	$r_{\text{eff}} = 21.86 \text{ nm}$		$b = 22.39 \text{ nm}$	

6 main resonance peaks in fig. 2(b), roughly in line with the dipole-dipole approximation results [25]. When the E_x polarized field is added (shown as green bars in fig. 2), it is observed that the resonance capacity for strong resonance is distributing from a 1-peaked structure at $s = -0.2$ for $28 * 28 * 12 \text{ nm}^3$ to a 6-peaked structure for $28 * 28 * 28 \text{ nm}^3$ or $28 * 28 * 44.8 \text{ nm}^3$. While, for the E_z polarized field (shown as red bars in fig. 2), the resonance position is shifted from $s = -0.68$, via some mediate processes of multi-resonances, to $s = -0.15$ by increasing thickness z . It is also noted that for the E_z polarized field in $28 * 28 * 12 \text{ nm}^3$ (red bars in fig. 2(a)) and the E_x polarized field in $28 * 28 * 44.8 \text{ nm}^3$ (green bars in fig. 2(c)), there is a strong resonance at the region $s \in (-0.2, 0.0)$, which corresponds to a high negative and real value of the electric permittivity $\epsilon(r, \omega)$. Therefore, we have found the resonance capacity distributions of a set of rectangular structures by varying the height and field polarization. If there is a large spatial extension in the field polarized direction and squeezing in the perpendicular direction, then resonance positions are shifted to the region $s \in (-0.2, 0.0)$ (to which the dielectric constants of

noble metals can access at this wavelength) and only one main peak exists. Finally, for the reference to the Au and Ag experiments in the visible, in table 2, we have designed a set of nanostrips at $\lambda = 632.8 \text{ nm}$ with strong surface plasmon resonances. We also compared our results with the discrete dipole approximation results [26] in table 3. Instead of the nanorods, here we have calculated the same volume nanostrips with small tubers at two tips, and found that there is a 20–50 nm difference in resonant wavelength, which means a good agreement between the two methods.

The immunity of the resonance capacity distribution to the wavelength in the subwavelength structures is also discussed. One characteristic is that, for a definite structure, its resonance capacity distribution is not varied with the volume zoomed in or out in a subwavelength region $l < \frac{\lambda}{15}$. The numerical calculations clearly indicate that the resonance positions and capacity are the same for a set of subwavelength cubes from $[12 \text{ nm}]^3$ to $[40 \text{ nm}]^3$, as shown in fig. 2(b), due to the quasistatic situation $l \ll \lambda$. Except for the cubic shape, we have checked several other shape structures, if their volume

is zoomed in or out in the subwavelength scale, this point also comes into existence. Another characteristic of immunity is that the resonance capacity distribution has only a small variation with increasing wavelength. As shown in fig. 3, for a $60 \times 20 \times 20 \text{ nm}^3$ nanostrip, when the incident wavelength is changed from $\lambda = 500 \text{ nm}$ to $\lambda = 632.8 \text{ nm}$, the position of surface plasmon resonances only has a small shift from $s = -0.0775 (\epsilon(r, \omega) = -11.90)$ to $s = 0.0825 (\epsilon(r, \omega) = -10.43)$. This point is very helpful in designing plasmonic nanostructures of noble metals in the visible. From $\lambda = 500 \text{ nm}$ to $\lambda = 632.8 \text{ nm}$, the dielectric constant of Au is within the region $(-2.42, -12.11)$, shown as yellow bars in fig. 3, while for Ag, the dielectric constant region is $(-9.56, -18.64)$, as gray bars in fig. 3 (the heights of these yellow and gray bars are not the calculation results, and only to guide one's eyes) [24]. In the figure, by adjusting the incident wavelength, the gold surface plasmon resonance region $(-2.42, -12.11)$ overlaps the theoretical prediction $(-10.43, -11.90)$, as well as the silver region $(-9.56, -18.64)$. Considering the metal loss, the suitable wavelength for an Ag nanostrip to perform the surface plasmon resonance experiments is near $\lambda = 532 \text{ nm}$; while for an Au nanostrip, this wavelength is near $\lambda = 632.8 \text{ nm}$. Finally, rather than the nanostructure in the visible, the Green's matrix method can be used to deal with the arbitrary shaped subwavelength structures in a wide spectral region.

In conclusion, the Green's matrix method has been developed, and a new physical variable, the resonance capacity of surface plasmon, has been introduced to quantitatively measure the electromagnetic energy gathering. For a certain structure type, the regulations of the resonance capacity can be obtained, so it is possible to tailor the resonant properties of metallic structure. As an example, series of thin nanostrips which are suitable to do some surface plasmon resonance experiments of Au and Ag in the visible have been designed. The resonance capacity of the subwavelength structure is found to be immune to the incident wavelength in the subwavelength scale. The method provides a powerful tool for plasmonic optics and the design of the subwavelength plasmonic structure.

This work was supported by the National Natural Science Foundation of China under Grants Nos. 10674009, 10521002, 10434020 and the National Key Basic Research Program No. 2007CB307001. YG is grateful for the visit

of the Abdus Salam International Center for Theoretical Physics (ICTP) and the useful discussions with Drs XIAOYONG HU, ZHENG LIU and ZHI LI.

REFERENCES

- [1] GIRARD C. and DEREUX A., *Rep. Prog. Phys.*, **59** (1996) 657.
- [2] GIRARD C. *et al.*, *Rep. Prog. Phys.*, **63** (2000) 893.
- [3] BOARDMAN A. D., *Electromagnetic Surface Modes* (John Wiley & Sons Ltd.) 1982.
- [4] RAETHER H., *Surface Plasmons* (Springer-Verlag, Berlin Heidelberg) 1988.
- [5] ZAYATS A. V. *et al.*, *Phys. Rep.*, **408** (2005) 131.
- [6] WOKAUN A. *et al.*, *Phys. Rev. Lett.*, **48** (1982) 957.
- [7] MUHLSCHLEGEL P. *et al.*, *Science*, **308** (2005) 1607.
- [8] WOKAUN A. *et al.*, *Phys. Rev. B*, **24** (1981) 849.
- [9] KIM E. M. *et al.*, *Phys. Rev. Lett.*, **95** (2005) 227402.
- [10] DANCKWERTS M. and NOVOTNY L., *Phys. Rev. Lett.*, **98** (2007) 026104.
- [11] MAIER S. A., KIK P. G. and ATWATER H. A., *Appl. Phys. Lett.*, **81** (2002) 1714.
- [12] MITSUI K., HANDA Y. and KAJIKAWA K., *Appl. Phys. Lett.*, **85** (2004) 4231.
- [13] WANG T. J. and LIN W. S., *Appl. Phys. Lett.*, **89** (2006) 173903.
- [14] MARTIN O. J. F., GIRARD C. and DEREUX A., *Phys. Rev. Lett.*, **74** (1995) 526.
- [15] GU Y., YU K. W. and SUN H., *Phys. Rev. B*, **59** (1999) 12847.
- [16] MORSE P. M. and FESHBACH H., *Methods of Theoretical Physics* (McGraw-Hill, New York) 1953.
- [17] ECONOMOU E. N., *Green's Functions in Quantum Physics*, 2nd edition (Springer, Berlin) 1990.
- [18] MARTIN O. J. F. and PILLER N. B., *Phys. Rev. E*, **58** (1998) 3909.
- [19] PAULUS M., GAY-BALMAZ P. and MARTIN O. J. F., *Phys. Rev. E*, **62** (2000) 5797.
- [20] SONDERGAARD T. and TROMBORG B., *Phys. Rev. B*, **66** (2002) 155309.
- [21] KOTTMANN J. P. and MARTIN O. J. F., *IEEE Trans. Antennas Propag.*, **48** (2000) 1719.
- [22] YAGHJIAN A. D., *Proc. IEEE*, **68** (1980) 248.
- [23] KREIBIG U. and VOLLMER M., *Optical Properties of Metal Clusters* (Springer-Verlag, Berlin, Heidelberg) 1995, pp. 26–35.
- [24] JOHNSON P. B. and CHRISTY R. W., *Phys. Rev. B*, **6** (1972) 4370.
- [25] FUCHS R., *Phys. Rev. B*, **11** (1975) 1732.
- [26] JAIN P. K. *et al.*, *J. Phys. Chem. B*, **110** (2006) 7238.